

Electron attachment and detachment: C₆F₆

Thomas M. Miller^{a,*}, Jane M. Van Doren^b, A.A. Viggiano^{a,1}

^a Air Force Research Laboratory, Space Vehicles Directorate, Hanscom Air Force Base, Bedford, MA 01731-3010, USA

^b Department of Chemistry, College of the Holy Cross, Worcester, MA 01610-2395, USA

Received 29 September 2003; accepted 7 November 2003

Abstract

Electron attachment to C₆F₆ is especially interesting because of the large change in symmetry between the neutral (D_{6h}) and anion (C_{2v}). We have made measurements of rate constants for electron attachment to C₆F₆ and thermal electron detachment from the parent anion, C₆F₆[−], over the temperature range 297–400 K, in 133 Pa of He gas. A flowing-afterglow Langmuir probe (FALP) apparatus was used for this work. At 298 K, the electron attachment rate constant is $k_a = 8.6 \pm 3.0 \times 10^{-8} \text{ cm}^3 \text{ s}^{-1}$, and the detachment rate constant k_d is approximately 35 s^{-1} . As the temperature increases k_d increases rapidly, to about 3000 s^{-1} at 400 K. The attachment/detachment equilibrium implies that the electron affinity of C₆F₆ is $0.53 \pm 0.05 \text{ eV}$. Density functional calculations were carried out in order to obtain thermal quantities needed to convert the equilibrium constant k_a/k_d into EA(C₆F₆). G3(MP2) calculations yielded an electron affinity of 0.454 eV. The fluoride affinity of C₆F₆ was calculated to be 1.26 eV at 298 K using this same method. We expect the G3(MP2) results to be good within 0.1 eV.

© 2004 Elsevier B.V. All rights reserved.

Keywords: Electron attachment; Electron detachment; Electron affinity; Flowing-afterglow Langmuir probe technique

1. Introduction

Hexafluorobenzene (C₆F₆) has an interesting and contentious history in regard to the formation of the parent anion in gases. An early tandem mass spectrometer measurement of the electron affinity gave EA(C₆F₆) = $1.8 \pm 0.3 \text{ eV}$ [1], and this result mislead later experimenters in the interpretation of their electron attachment data at elevated temperatures. To make matters worse, experiments conducted a few years later placed EA(C₆F₆) > 1.6 eV [2] and < 1.8 eV [3]. In 1984, Adams et al. [4] and Spyrou and Christophorou [5] observed what appeared to be an unprecedented and dramatic decrease in the rate constant for electron attachment to C₆F₆ with temperature, which would imply a negative (unphysical) activation energy for electron attachment. Chen et al. [6] then explained the conundrum by pointing out results obtained at about the same time in an electron capture detector: C₆F₆[−] was thermally detaching the extra electron at elevated temperatures, at a rate that implied an EA of $0.86 \pm 0.03 \text{ eV}$ [7]. This explanation was not immediately

accepted [8], mainly because of the seemingly high EA of C₆F₆, even considering the new value of 0.86 eV.

Shortly afterwards, in 1986, Chowdhury et al. used high-pressure mass spectrometry to measure EA(C₆F₆) and found $0.52 \pm 0.10 \text{ eV}$ [9–11] and noted that thermal detachment would take place at modest temperatures. In 1992, Knighton et al. [12] confirmed the electron detachment explanation of the previous experiments and measured rate constants for the detachment process over the temperature range 307–349 K. Much of the Knighton et al. work regarded the role of unavoidable oxygen impurities in high-pressure experiments; they concluded that high-pressure experiments carried out without mass spectrometric analysis of the ions, such as those of Spyrou and Christophorou [5] and Chen et al. [6], were unlikely to be correctly interpreted. In a later work, reactions between O₂[−] and C₆F₆ were found to be collisional and led to fragmentation of the C₆F₆ in 92% of the reactions, creating more stable ions in the process [13]. Reactions between C₆F₆[−] and O₂ were 50 times slower and led to total rearrangement of the reactants [13]. The story does not end here. In 1994, Chen et al. [14] repeated the C₆F₆ electron capture detector experiment and obtained EA(C₆F₆) = $0.83 \pm 0.22 \text{ eV}$ from mass-analyzed C₆F₆[−] ion signals. In 1995, Christophorou and Datskos [15] used the time-resolved electron swarm technique, with

* Corresponding author.

E-mail addresses: Thomas.Miller@hanscom.af.mil (T.M. Miller), viggiano@plh.af.mil (A.A. Viggiano).

¹ Tel.: +1-781-377-4028; fax: +1-781-377-7091.

high pressures of N_2 buffer gas, to measure rate constants for both electron attachment to C_6F_6 and detachment from $C_6F_6^-$ at mean electron energies from 0.2 to 1.0 eV and temperatures from 300 to 575 K. An Arrhenius plot of the detachment rate constants yielded an activation energy of 0.477 eV, which was taken as an estimate of $EA(C_6F_6)$. Around that same time, Nakajima et al. reported a photoelectron energy spectrum for $C_6F_6^-$ which they interpreted as giving $EA(C_6F_6) \leq 0.80 \pm 0.10$ eV [16]. Recently, Chen and Chen [17] have interpreted electron capture detector data as yielding three electronic states of $C_6F_6^-$, with electron binding energies of 0.80, 0.70, and 0.55 eV. However, similar work [18,19] on NO and O_2 from Chen's laboratory flies in the face of well-established spectroscopic results and is clearly wrong. This point has been forcefully made by Ervin et al. [20], who concluded that "all electron capture detector measurements of electron affinities should be considered subject to large and unknown errors."

We have omitted in this history the common complaint of one author to another that the other's $C_6F_6^-$ ions must have been in an excited state, an objection aimed at any experiment supporting a lower value of $EA(C_6F_6)$ than accepted by the complainant. It seems to us that in all of the experiments the buffer gas pressure was high enough that the neutrals and anions—whatever they were—were in thermal equilibrium with the buffer gas. The flowing-afterglow Langmuir probe (FALP) experiment reported here, and that of Adams et al. [4], carried out in low-pressure He gas, has the weakest claim along this line [21], but the FALP results have been consistently found in agreement with accurate EA measurements [22], the gas purity is easy to maintain, the ion products of attachment are routinely mass analyzed, and the reactant concentration is generally so low that ion–molecule reactions are not an issue in the mass spectrum. We are therefore reporting here results for electron attachment to C_6F_6 and detachment from $C_6F_6^-$, and the implications in terms of $EA(C_6F_6)$. As shown in Ref. [23], rate constants for electron detachment do not strictly follow Arrhenius behavior. In the present work, we will account for entropy changes, including the important rotational symmetry numbers, and the integrated specific heats of C_6F_6 and $C_6F_6^-$, in determining $EA(C_6F_6)$. Furthermore, we have carried out density functional and G3(MP2) calculations of $EA(C_6F_6)$.

The electron-beam experiments of Ingólfsson and Illenberger [24] are illuminating in understanding electron attachment to C_6F_6 because they showed (as one might guess from the thermal experiments) that the attachment takes place via a narrow zero-energy resonance, signifying electron capture into a nuclear-excited Feshbach resonant state of the anion, in the continuum. The electron energy may then be taken up by internal modes of the C_6F_6 , staving off autodetachment long enough for radiative or collisional stabilization. At electron energies well above those accessed in thermal experiments, the electron-beam experiments recorded the opening of endothermic dissociative attachment channels.

2. Experimental method

A FALP apparatus was used for this work at the Air Force Research Laboratory. Both the method [25] and this particular apparatus [26] have been well described in the literature and will not be detailed here. The measurements were carried out in 133 Pa of He gas. The C_6F_6 gas [27] was introduced into the flow tube at a concentration of typically 400 ppbv. An example of the data obtained is shown in Fig. 1. Data such as these were fit to determine the electron attachment rate constant k_a and the detachment rate constant k_d . The results at each temperature are given in Table 1. At the same time, we measured the attachment rate constant for SF_6 at 298 K and obtained $2.26 \times 10^{-7} \text{ cm}^3 \text{ s}^{-1}$, which agrees with the accurate value $2.27 \pm 0.07 \times 10^{-7} \text{ cm}^3 \text{ s}^{-1}$ (at 295 K) [28].

As outlined in Ref. [29], and illustrated in Fig. 1, the electron density plot is characteristic of an electron-detaching plasma when the curve reaches a diffusion-limited steady-state condition at long times. The early part of the electron density curve is controlled by k_a . The level of the late portion of the curve is determined by the ratio k_d/k_a . The optimum temperature for determining k_d is that for which the attachment frequency $\nu_a = k_a n_r$ is comparable in magnitude to k_d (both in units of s^{-1}), but larger than the ambipolar diffusion decay constant ν_D (the latter being measured in absence of reactant gas), otherwise the plasma diffuses away before the steady-state condition is reached. Values of ν_D are included in Table 1 for comparison to k_d . (Values of ν_D may vary in different experiments because of the small amount of Ar gas added to the He.) We note that the results are dependent only on relative values of the electron density as long as the initial electron number density

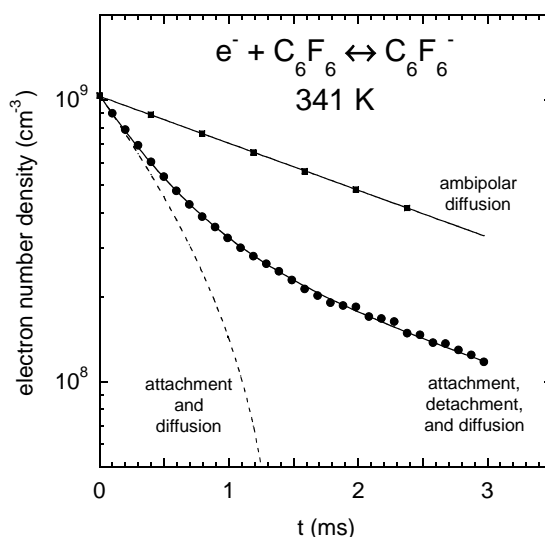


Fig. 1. An example of the FALP data obtained for C_6F_6 , at 341 K, with a concentration of C_6F_6 of $1.13 \times 10^{10} \text{ cm}^{-3}$. The upper solid line was obtained without C_6F_6 and gave $\nu_D = 397 \text{ s}^{-1}$. The fit to the lower data set yielded $k_a = 9.8 \times 10^{-8} \text{ cm}^3 \text{ s}^{-1}$ and $k_d = 982 \text{ s}^{-1}$.

Table 1
Rate constants for electron attachment (k_a) to C_6F_6 and electron detachment (k_d) from $C_6F_6^-$

T (K)	k_a ($10^{-8} \text{ cm}^3 \text{ s}^{-1}$)	k_d (s^{-1})	ν_D (s^{-1})	EA (eV)
297	10.0	(104)	355	–
	7.0	(30)	355	–
299	8.5	(35)	385	–
	8.8	(30)	385	–
320	8.0	372	379	(0.505)
341	9.2	820	397	0.520
	9.8	982	397	0.516
350	7.0	890	443	0.523
	7.0	918	443	0.522
	7.8	985	431	0.523
	7.0	960	425	0.521
	8.1	990	417	0.524
360	7.9	1360	439	0.529
362	9.5	1730	398	0.531
370	7.9	1780	420	0.536
	7.9	1850	420	0.535
	7.9	1730	420	0.537
	7.9	1600	446	0.539
373	5.8	1880	434	0.529
	6.1	1880	434	0.530
400	(3.8)	(3000)	479	(0.537)

The experimental uncertainty is $\pm 35\%$ except that the k_d in parentheses are not reliable since they are much smaller than the ambipolar diffusion rate, but give the best fit to the data. At 400 K the concentration of C_6F_6 is high enough that the reaction reaches steady state in such a short time as to be deemed similarly less accurate. For comparison with k_d , the measured ambipolar diffusion decay constant ν_D is given. The final column gives the apparent value of EA(C_6F_6) derived from the data using Eq. (1).

(at the reactant port) is much smaller than the reactant concentration, n_r . That is, changing the initial electron density simply moves the curve in Fig. 1 up or down, but does not change its shape. Furthermore, we note that the results for k_d are independent of n_r since k_d is a unimolecular rate constant. In the C_6F_6 case, these considerations mean that at 298 K the data give k_a accurately but not k_d . By 320 K, k_d is approximately the same magnitude as ν_D , giving the electron density curve an exponential appearance as electron detachment tends to cancel the effect of diffusion. At higher temperatures, this curve looks as in Fig. 1. At still higher temperatures where k_d is much greater than ν_a , the electron density curve is practically indistinguishable from the diffusion curve because the C_6F_6 molecules have so much internal energy that the extra electron cannot remain attached long enough to have any effect on the electron density. At 400 K, we must use such high concentrations of C_6F_6 ($8 \times 10^{10} \text{ cm}^{-3}$) that the steady-state condition is reached in such a short time that it becomes difficult to determine k_a and k_d accurately. Thus, the detachment process may be studied with the FALP apparatus only over a 50–80 °C temperature range.

We have earlier given the details of obtaining the EA of the reactant from the equilibrium constant k_a/k_d [29]. The equilibrium constant yields the free energy, ΔG° . To obtain the enthalpy ΔH° , the entropy of reaction must be known.

Then, the EA may be obtained by using integrated heat capacities to reduce $-\Delta H^\circ$ from the measured temperature T to 0 K. The necessary entropies and integrated heat capacities must be measured, estimated, or calculated. Their effect is usually not large—several tens of meV—but significant in determining EAs which are only some hundreds of meV. In Ref. [29], we made several approximations to obtain entropies and integrated specific heats. Since then, it has become possible to routinely calculate the needed corrections [22] and thus present a more accurate value for the EA of the reactant.

3. Computational method and results

The G3(MP2) method [30] was applied to C_6F_6 and $C_6F_6^-$ in order to obtain EA(C_6F_6) for comparison with the experimental result. The method is accurate on average within 56 meV for a large test set of molecules of accurately known properties [30]. In our experience, it is rare for the G3(MP2) EA to be wrong by more than 100 meV [31]. Density functional theory (DFT) was applied to these molecules in order to obtain entropy and heat capacity quantities needed to correctly interpret the FALP data in terms of EA(C_6F_6). DFT is expected to provide these quantities more accurately than the Hartree–Fock (HF) method built into the G3(MP2) prescription because electron correlation is approximately accounted for in the DFT functionals and because a larger basis set may be used than is specified for the HF portion of the G3(MP2) prescription. But the DFT EAs tend to be 0.2–0.5 eV too high, depending on the basis set used. The Gaussian-03W program package was used for both the G3(MP2) and DFT work described here [32]. The stability of the wavefunctions used was checked in each case, i.e., it was verified that the molecular orbital set chosen led to the lowest energy wavefunction.

The G3(MP2) formalism uses the HF method to obtain zero-point energies (ZPE) and thermal energy adjustments to enthalpies and free energies, with harmonic vibrational frequencies scaled by 0.8929. High-level energy calculations are carried out on a much better geometry obtained using second-order Møller–Plesset perturbation theory (MP2) with the 6-31G(d) basis set on all electrons. As occasionally happens using the GX methods, the HF geometry for $C_6F_6^-$ has less symmetry than does the MP2 geometry, so the ZPE for the anion is not strictly correct, but only differences in the ZPE enter the EA(C_6F_6) result. The DFT calculations indicated that the ZPE issue affects EA(C_6F_6) at the 17 meV level. The high-level G3(MP2) calculations were carried out for D_{6h} C_6F_6 and C_{2v} $C_6F_6^-$, after the MP2(Full)/6-31G(d) optimization procedure showed that these structures were the correct ones.

The DFT calculations were performed using the B3LYP hybrid functional [33] and the 6-31+G(3df) basis set [34]. Calculated harmonic vibrational frequencies were scaled by 0.989 [35]. Entropies (with molecular symmetries given

Table 2

Results of Møller–Plesset and density functional calculations for C_6F_6 (D_{6h} , $^1A_{1g}$) and $C_6F_6^-$ (C_{2v} , 2A_1)

Quantity	G3(MP2)		DFT	
	C_6F_6	$C_6F_6^-$	C_6F_6	$C_6F_6^-$
S_{350}° (meV K^{-1}) ^a	4.258	4.758	4.228	4.686
$\int^{350} C_p dT$ (eV) ^a	0.352	0.382	0.345	0.376
Zero-point energy ^a	0.05014	0.04558	0.05131	0.04614
Total energy (0 K) ^b	−826.75105	−826.76772	−827.64929	−827.67455
EA (eV) ^b	0.454	–	0.687	–
r (C^A-C^B) ^c	1.391	1.405	1.392	1.402
r (C^B-C^B) ^c	1.391	1.372	1.392	1.372
r (C^A-F^A) ^c	1.340	1.403	1.340	1.393
r (C^B-F^B) ^c	1.340	1.390	1.340	1.374
$\angle(C^B-C^A-C^B)$	120.0	117.5	120.0	118.2

The zero-point and total energies are in hartree units. The bond lengths are in Å units. The entropy S_{350}° and the integrated specific heat $\int^{350} C_p dT$ are evaluated at 350 K for interpretation of 350 K electron attachment data.

^a HF/6-31G(d) level of theory, scaled by 0.8929, for G3(MP2) results and B3LYP/6-31+G(3df) level of theory, scaled by 0.989, for DFT results.

^b G3(MP2) formalism and B3LYP/6-31+G(3df)//B3LYP/6-31+G(3df) + ZPE for DFT results.

^c MP2(Full)/6-31G(d) for G3(MP2) results and B3LYP/6-31+G(3df) for DFT results. Superscript A denotes two special C and F atoms at opposite ends of the anion (positions 1 and 4); see text and Fig. 2. Superscript B denotes the remaining C and F atoms (positions 2, 3, 5, 6). A and B are indistinguishable in the neutral.

above) and integrated heat capacities were calculated at each temperature for which reliable k_d rate constants were obtained. Values calculated at 350 K are included in Table 2 along with total energies and several geometry parameters. Though not shown explicitly in Table 2, we note that the vibrational entropy change between C_6F_6 and $C_6F_6^-$ is about 50% greater than the rotational entropy change, even with the large change in rotational symmetry number. The DFT EA(C_6F_6) is also given in Table 2, though experience has been that it will be 0.25 eV too high for the basis set used here [36]. A thorough study of DFT methods for determining EAs has been published by Rienstra-Kiracofe et al. [37].

Aromatic C_6F_6 is obviously completely planar with D_{6h} symmetry. The most visible feature of the calculated anion structure is that two opposite F atoms (at positions 1 and 4) protrude above the average carbon plane by about 23° . The C atoms to which these two F atoms are bound lie very slightly below the plane in which the remaining four C atoms lie, with a dihedral angle (1, 2, 3, 4) of -0.5° . The remaining four F atoms lie in a plane of their own, slightly below that of the four planar C atoms (positions 2, 3, 5, and 6). Some of the relevant geometrical parameters are given in Table 2, and the $C_6F_6^-$ structure is shown in Fig. 2. The HF structure for $C_6F_6^-$ has the F atom at position 1 protruding further out of the average carbon plane than the F atom at position 4.

The C_{2v} anion structure given here is consistent with that calculated 20 years ago by Shchegoleva et al. [38] and with that calculated by Hiraoka et al. [39]. It is different from that deduced from an ESR spectrum [40], as discussed in Ref. [38].

The G3(MP2) energy of $C_6F_7^-$ was also calculated (−926.56307 hartree at 0 K and −926.55044 hartree at 298 K), from which obtains the fluoride affinity of C_6F_6 , 1.24 eV (0 K) or 1.26 eV (298 K). These values are in rea-

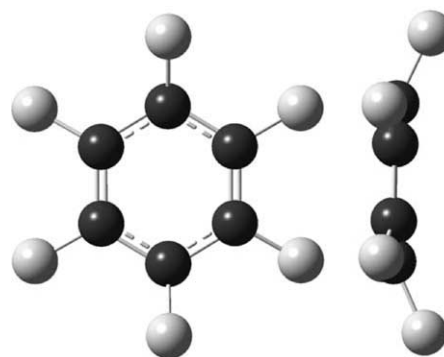


Fig. 2. Views of the C_{2v} $C_6F_6^-$ anion ring. Left: from above the ring. Right: from the side. F atoms at positions 1 and 4 protrude out of the average carbon plane. The other F atoms protrude in the opposite direction, but much less so.

sonable agreement with the experimental result of Hiraoka et al. [41], 1.2 eV (no uncertainty given).

4. Discussion

We note that the symmetry change between C_6F_6 and $C_6F_6^-$ plays an important role in the attachment/detachment process. Neutral C_6F_6 has D_{6h} symmetry (with a rotational symmetry number of 12), while the anion has C_{2v} symmetry (with a rotational symmetry number of 2). This degree of change is highly unusual, and the concomitant effect on the entropy change in electron attachment is important in the conversion from a measured equilibrium constant to an EA value. Another way of looking at this is to say that if there were no change in symmetry between C_6F_6 and $C_6F_6^-$, the detachment rate constant would be 5.6 times larger than observed at 350 K!

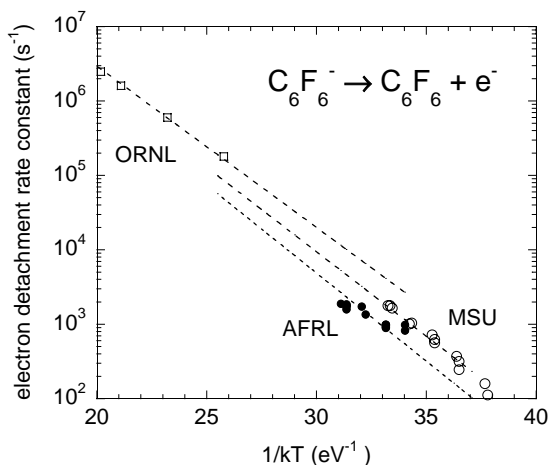


Fig. 3. A comparison of electron detachment rate constants k_d for C_6F_6^- . AFRL: present results. ORNL: Christophorou and Datskos [15]. MSU: Knighton et al. [12].

The measured k_a value ($8.6 \pm 3.0 \times 10^{-8} \text{ cm}^3 \text{ s}^{-1}$ at 298 K), falls slightly lower than that measured by Adams et al. [4] using the same method; they obtained $1.1 \pm 0.2 \times 10^{-7} \text{ cm}^3 \text{ s}^{-1}$ at 300 K. Spyrou and Christophorou [5] measured a similar value at their lowest mean electron energy of 0.055 eV and gas temperature of 300 K, at high pressures of N_2 . According to the electron capture model of Klots [42], this k_a represents about one negative ion formed in every three collisions between C_6F_6 and an electron.

In Fig. 3, the present results for k_d (obtained in 133 Pa He gas) are compared to those of Knighton et al. [12] (obtained in 67 Pa CH_4 gas) and those of Christophorou and Datskos [15] (obtained in 50–300 kPa N_2 gas). The latter results [15] correspond to mean electron energies above 0.2 eV, but the measured k_d appear to be independent of electron energy in the range 0.20–0.38 eV.

As shown in Ref. [29], the k_d follows a temperature dependence given by

$$k_d = k_a L_0 \left(\frac{273.15}{T} \right) \times \exp \left[- \left(\frac{\text{EA}}{kT} \right) - \left(\frac{\Delta S^\circ}{k} \right) - \left(\frac{H_T - H_0}{kT} \right) \right]. \quad (1)$$

The electron part of the entropy term ΔS° in the argument of the exponential contributes a factor of $T^{5/2}$ to k_d , so the leading temperature dependence becomes $T^{3/2}$. In Eq. (1), k is Boltzmann's constant, L_0 is Loschmidt's number, EA is the electron affinity of C_6F_6 (at 0 K, by definition), ΔS° is the entropy change due to electron attachment, and $H_T - H_0$ is the thermal energy correction needed to reduce the EA result to 0 K. The T dependence of k_d is thus complicated by that contained implicitly in other quantities such as k_a and the heat capacities of the neutral and anion. In the present case, k_a changes very little in the narrow temperature range accessible to us.

EA(C_6F_6) may be obtained from the measured k_a and k_d using the inverse of Eq. (1), with details given in Ref. [29] in terms of ΔG° and ΔH° . An example will be given for the 350 K data, using the average values from Table 1 of $k_a = 7.38 \times 10^{-8} \text{ cm}^3 \text{ s}^{-1}$ and $k_d = 949 \text{ s}^{-1}$. The B3LYP/6-31+G(3df) DFT calculations yielded entropy and integrated heat capacity values for $\text{D}_{6h} \text{C}_6\text{F}_6$ and $\text{C}_{2v} \text{C}_6\text{F}_6^-$ as given in Table 2. The entropy change is

$$\Delta S^\circ = S(\text{anion}) - S(\text{neutral}) - S(\text{electron}), \quad (2)$$

$$\Delta S^\circ = 4.686 - 4.228 - 0.251 \text{ meV K}^{-1} \text{ at } 350 \text{ K} \quad (3)$$

for a net entropy change of 0.207 meV K^{-1} . The integrated heat capacities needed to convert the “EA” at 350 K to a true EA (at 0 K) are

$$H_T - H_0 = \int_0^T C_p(\text{electron}) dT + \int_0^T C_p(\text{neutral}) dT - \int_0^T C_p(\text{anion}) dT, \quad (4)$$

$$H_T - H_0 = 75 + 345 - 376 \text{ meV at } 350 \text{ K}. \quad (5)$$

Thermochemical quantities for the electron are expressed using Boltzmann statistics for reasons laid out in the JANAF tables [43]. The net change in integrated heat capacity is 45 meV at 350 K. The final result using these figures in Eq. (1) is EA(C_6F_6) = 523 meV. (Other thermochemical quantities with these numbers are $\Delta G^\circ = -640 \text{ meV}$ and $\Delta H^\circ = -567 \text{ meV}$ at 350 K.) Similar analysis of all data for which optimum conditions obtain (ν_a comparable to k_d and both larger than ν_D) give us an average value EA(C_6F_6) = $0.53 \pm 0.05 \text{ meV}$. The uncertainty was determined by letting k_a and k_d take extreme values and including additional estimated uncertainty in the temperature, and consideration of possible errors in the calculated entropy and heat capacity adjustments. Since EA has only a logarithmic dependence on the ratio of k_a to k_d , EA is rather insensitive to errors in these quantities. Accuracy in the temperature measurement is important, but is easier to attain. Errors in the calculated entropies and integrated heat capacities affect EA at the fraction-of-an-meV level. To test the accuracy of the computed quantities, DFT entropy calculations for F_2 , C_2F_4 , and SF_6 were compared to those in the JANAF tables [43]. Generally speaking, we found that the larger the molecule, the better the agreement between DFT and JANAF. For SF_6 , the calculated entropy results are good within 2% in the temperature range of the present data, and the calculated integrated heat capacity agreed within 9%. Only differences between neutral and anion entropies and integrated heat capacities enter into the present EA determination, and these differences amount to 1/10th of the individual values. Hence, the error in the thermal adjustments is only about 1%. Furthermore, these adjustments amount to only 1/5th of the EA value. Thus, uncertainties in the calculated thermal adjustments are negligible insofar as EA(C_6F_6) is concerned.

If one knows EA, then k_d values calculated using that EA are extremely sensitive to inaccuracy in EA. In Fig. 3, the dashed lines are evaluations of Eq. (1) which pass through each of the three available data sets. The line passing through the present (AFRL) data uses EA = 530 meV; that for the ORNL data [15] uses EA = 483 meV; and that for the MSU data [12] uses EA = 507 meV. All three lines were calculated using our 298 K value of k_a , $8.6 \times 10^{-8} \text{ cm}^3 \text{ s}^{-1}$, and entropies and heat capacities calculated using density functional theory. These entropies and heat capacities are, of course, temperature dependent, but the net effect on the argument of the exponential in Eq. (1) changes by only 47 meV over the 309–575 K range of the data in Fig. 3. At the time the ORNL and MSU data were published, those authors used a value of k_a of $1.0 \times 10^{-7} \text{ cm}^3 \text{ s}^{-1}$ to assess the data. If we recalculate the dashed lines in Fig. 3 using this higher value of k_a , the EA values must be raised slightly (by 10 meV for ORNL and by 3 meV for MSU data) in order to make the lines pass through the centroid of the respective data sets. All of these apparent EA values are within the ± 50 meV uncertainty estimated for the 530 meV EA deduced from the present attachment/detachment experiment.

To summarize, the experiment strictly speaking measures ΔG° at each temperature. The determination of EA(C_6F_6) depends on entropy and heat capacity quantities which must be found elsewhere. The entropy and integrated heat capacity for the electron are accurate within Boltzmann statistics [43]. The entropy and integrated heat capacities for C_6F_6 and C_6F_6^- partially cancel except for the known effects of electron spin degeneracy and rotational symmetry number. The quantities calculated using DFT introduce a 54 meV improvement over what one would estimate without the calculated quantities, as was done in Ref. [29]. Uncertainty in the calculated quantities affects the EA determination below the meV level, so it is appropriate to consider our EA(C_6F_6) = 0.53 ± 0.05 eV result as an experimental one.

5. Conclusions

We have made measurements of rate constants for electron attachment to C_6F_6 and thermal electron detachment from the parent anion, C_6F_6^- , over the temperature range 298–400 K, in 133 Pa of He gas, in an FALP apparatus. At 298 K, the electron attachment rate constant is $k_a = 8.6 \pm 3.0 \times 10^{-8} \text{ cm}^3 \text{ s}^{-1}$, and the detachment rate constant k_d is approximately 35 s^{-1} . This value of k_a is slightly lower than previous work [4,5], but is in agreement within error limits. As the temperature increases k_d increases rapidly, to a value of about 3000 s^{-1} at 400 K. The large change in symmetry between C_6F_6 and C_6F_6^- , from D_{6h} to C_{2v} , is found to suppress the detachment process from what one would guess based solely on the low electron affinity. The attachment/detachment equilibrium implies that the electron affinity of C_6F_6 is 0.53 ± 0.05 eV. Density functional calculations were carried out in order to obtain entropies and heat

capacities needed to convert the equilibrium constant k_a/k_d into EA(C_6F_6). Higher level G3(MP2) calculations yielded an electron affinity of 0.454 eV and a fluoride affinity for C_6F_6 of 1.26 eV at 298 K. In our experience, the G3(MP2) results are good within 0.1 eV.

Note added in proof

While this publication was in press, a thorough theoretical study of the C_6F_6 anion appeared [44] which agrees with the present conclusions regarding the C_{2v} , 2A_1 nature of the anion. We should also mention the pulse-radiolysis study of electron attachment to C_6F_6 in 4–14 kPa Xe, by H. Shimamori et al. [45].

Acknowledgements

We dedicate this work to our friend Prof. Dr. Tilmann Märk. Our paths have crossed often with electron attachment projects and conferences. Under his leadership the productive Ion Physics Institute at the University of Innsbruck has become an inspiring place to visit.

We are grateful for the support of the Air Force Office of Scientific Research for this work. J.M.V.D. was a National Academy of Sciences Senior Visiting Fellow during the time of this work. T.M.M. is under contract (F19628-99-C-0069) with Visidyne, Inc., Burlington, MA, USA.

References

- [1] C. Lifshitz, T.O. Tiernan, B.M. Hughes, J. Chem. Phys. 59 (1973) 3182.
- [2] L.J. Rains, H.W. Moore, R.T. McIver Jr., J. Chem. Phys. 68 (1978) 3309. The relative EA scale in this paper proves to be correct except for the placements of the anchor molecule and of tetrafluoroquinone.
- [3] R.N. McDonald, A.K. Chowdhury, D.W. Setser, J. Am. Chem. Soc. 103 (1981) 7586. The limit on EA(C_6F_6) found in this paper is correct.
- [4] N.G. Adams, D. Smith, E. Alge, J. Burdon, Chem. Phys. Lett. 116 (1985) 460.
- [5] S.M. Spyrou, L.G. Christophorou, J. Chem. Phys. 82 (1985) 1048.
- [6] E.C.M. Chen, W.E. Wentworth, T. Limero, J. Chem. Phys. 83 (1985) 6541.
- [7] N. Hernandez-Gil, W.E. Wentworth, T. Limero, E.C.M. Chen, J. Chromatogr. 312 (1984) 31.
- [8] L.G. Christophorou, J. Chem. Phys. 83 (1985) 6543.
- [9] S. Chowdhury, E.P. Grimsrud, T. Heinis, P. Kebarle, J. Am. Chem. Soc. 108 (1986) 3630.
- [10] S. Chowdhury, T. Heinis, E.P. Grimsrud, P. Kebarle, J. Phys. Chem. 90 (1986) 2747.
- [11] G.W. Dillow, P. Kebarle, J. Am. Chem. Soc. 111 (1989) 5592.
- [12] W.B. Knighton, J.A. Bogner, E.P. Grimsrud, Chem. Phys. Lett. 192 (1992) 522. A more detailed version of the history of this problem is given in this reference, up to 1992.
- [13] W.B. Knighton, T.M. Miller, A.A. Viggiano, R.A. Morris, J.M. Van Doren, J. Chem. Phys. 109 (1998) 9632.
- [14] E.C.M. Chen, J.R. Wiley, C.F. Batten, W.E. Wentworth, J. Phys. Chem. 98 (1994) 88.

- [15] L.G. Christophorou, P.G. Datskos, *Int. J. Mass Spectrom. Ion Processes* 149/150 (1995) 59. An earlier report was given by P.G. Datskos, L.G. Christophorou, J.G. Carter, *J. Chem. Phys.* 98 (1993) 7875.
- [16] A. Nakajima, T. Taguwa, K. Hoshino, T. Sugioka, T. Ono, K. Watanabe, K. Nakao, Y. Konishi, R. Kishi, K. Kaya, *Chem. Phys. Lett.* 214 (1993) 22.
- [17] E.S. Chen, E.C.M. Chen, *J. Chromatogr. A* 952 (2003) 173.
- [18] E.S. Chen, W.E. Wentworth, E.C.M. Chen, *J. Mol. Struct.* 606 (2002) 1.
- [19] E.S. Chen, E.C.M. Chen, *J. Phys. Chem. A* 107 (2003) 169.
- [20] K.M. Ervin, I. Anusiewicz, P. Skurski, J. Simons, W.C. Lineberger, *J. Phys. Chem. A* 107 (2003) 8521.
- [21] D.H. Williamson, W.B. Knighton, E.P. Grimsrud, *Int. J. Mass Spectrom.* 195/196 (2000) 481.
- [22] T.M. Miller, A.A. Viggiano, A.E.S. Miller, *J. Phys. Chem. A* 106 (2002) 10200. In Table I of this reference, the plasma velocity should be given as 100 m s^{-1} .
- [23] J.M. Van Doren, S.A. McSweeney, M.D. Hargus, D.M. Kerr, T.M. Miller, S.T. Arnold, A.A. Viggiano, *Int. J. Mass Spectrom.* 228 (2003) 541.
- [24] O. Ingólfsson, E. Illenberger, *Int. J. Mass Spectrom.* 149/150 (1995) 79.
- [25] D. Smith, P. Španěl, *Adv. At. Mol. Phys.* 32 (1994) 307.
- [26] T.M. Miller, A.E.S. Miller, J.F. Paulson, X. Liu, *J. Chem. Phys.* 100 (1994) 8841.
- [27] The hexafluorobenzene was purchased from Sigma-Aldrich, and was stated to be 99.9% pure. Several freeze-pump-thaw cycles were applied to the liquid before preparing 0.2% C_6F_6 mixtures in He for introduction into the flow tube.
- [28] R.W. Crompton, G.N. Haddad, *Aust. J. Phys.* 36 (1983) 15; Z.L. Petrović, R.W. Crompton, *J. Phys. B: At. Mol. Phys.* 17 (1985) 2777.
- [29] T.M. Miller, R.A. Morris, A.E.S. Miller, A.A. Viggiano, J.F. Paulson, *Int. J. Mass Spectrom. Ion Processes* 135 (1994) 195.
- [30] L.A. Curtiss, P.C. Redfern, K. Raghavachari, V. Rassolov, J.A. Pople, *J. Chem. Phys.* 110 (1999) 4703.
- [31] T.M. Miller, S.T. Arnold, A.A. Viggiano, *Int. J. Mass Spectrom.* 227 (2003) 413; S.T. Arnold, T.M. Miller, A.A. Viggiano, *J. Phys. Chem. A* 106 (2002) 9900.
- [32] M.J. Frisch, G.W. Trucks, H.B. Schlegel, G.E. Scuseria, M.A. Robb, J.R. Cheeseman, J.A. Montgomery Jr., T. Vreven, K.N. Kudin, J.C. Burant, J.M. Millam, S.S. Iyengar, J. Tomasi, V. Barone, B. Menucci, M. Cossi, G. Scalmani, N. Rega, G.A. Petersson, H. Nakatsuji, M. Hada, M. Ehara, K. Toyota, R. Fukuda, J. Hasegawa, M. Ishida, T. Nakajima, Y. Honda, O. Kitao, H. Nakai, M. Klene, X. Li, J.E. Knox, H.P. Hratchian, J.B. Cross, C. Adamo, J. Jaramillo, R. Gomperts, R.E. Stratmann, O. Yazyev, A.J. Austin, R. Cammi, C. Pomelli, J.W. Ochterski, P.Y. Ayala, K. Morokuma, G.A. Voth, P. Salvador, J.J. Dannenberg, V.G. Zakrzewski, S. Dapprich, A.D. Daniels, M.C. Strain, O. Farkas, D.K. Malick, A.D. Rabuck, K. Raghavachari, J.B. Foresman, J.V. Ortiz, Q. Cui, A.G. Baboul, S. Clifford, J. Cioslowski, B.B. Stefanov, G. Liu, A. Liashenko, P. Piskorz, I. Komaromi, R.L. Martin, D.J. Fox, T. Keith, M.A. Al-Laham, C.Y. Peng, A. Nanayakkara, M. Challacombe, P.M.W. Gill, B. Johnson, W. Chen, M.W. Wong, C. Gonzalez, J.A. Pople, *Gaussian 03, Revision B.02*, Gaussian, Inc., Pittsburgh PA, 2003.
- [33] A.D. Becke, *J. Chem. Phys.* 98 (1993) 5648; J.P. Perdew, K. Burke, Y. Wang, *Phys. Rev. B* 54 (1993) 16533; K. Burke, J.P. Perdew, Y. Wang, in: J.F. Dobson, G. Vignale, M.P. Das (Eds.), *Electron Density Functional Theory: Recent Progress and New Directions*, Plenum, New York, 1998.
- [34] J.B. Foresman, Æleen Frisch, *Exploring Chemistry with Electronic Structure Methods*, 2nd ed., Gaussian, Pittsburgh, 1996.
- [35] C.W. Bauschlicher, H. Partridge, *J. Chem. Phys.* 103 (1995) 1788.
- [36] The DFT value for $\text{EA}(\text{C}_6\text{F}_6)$ was 0.852 eV using the basis set 6-31+G(d) for the geometry optimization and harmonic frequency analysis. $\text{EA}(\text{C}_6\text{F}_6)$ lowered to 0.733 eV with additional polarization functions [6-31+G(2d)], and lowered still further to 0.687 eV with higher polarization functions [6-31+G(3df)]. The G3(MP2) result is 0.454 eV.
- [37] J.C. Rienstra-Kiracofe, G.S. Tschumper, H.F. Schaefer, S. Nandi, G.B. Ellison, *Chem. Rev.* 102 (2002) 231.
- [38] L.N. Shchegoleva, I.I. Bilkis, P.V. Schastnev, *Chem. Phys.* 82 (1983) 343.
- [39] K. Hiraoka, S. Mizuse, S. Yamabe, *J. Phys. Chem.* 94 (1990) 3689.
- [40] C.R.M. Symons, R.C. Selby, I.G. Smith, S.W. Bratt, *Chem. Phys. Lett.* 48 (1977) 100.
- [41] K. Hiraoka, S. Mizuse, S. Yamabe, *J. Chem. Phys.* 86 (1987) 4102.
- [42] C.E. Klotz, *Chem. Phys. Lett.* 38 (1976) 61. The polarizability of C_6F_6 , 9.58 Å^3 , was taken from K.T. No, K.H. Cho, M.S. Jhon, H.A. Scheraga, *J. Am. Chem. Soc.* 115 (1993) 2005.
- [43] M.W. Chase, C.A. Davies, J.R. Downey, D.J. Frurip, R.A. McDonald, A.N. Syverud, *JANAF Thermochemical Tables*, 3rd ed.; *J. Phys. Chem. Ref. Data* 14 (Suppl. 1) (1986).
- [44] X.-J. Hou, M.-B. Huang, *J. Mol. Struct.* 638 (2003) 209.
- [45] H. Shimamori, T. Sunagawa, Y. Ogawa, Y. Tatsumi, *Chem. Phys. Lett.* 227 (1994) 609.